Experimental validation of a locally resonant metamaterial plate

Hernan Vazquez, Javier; Brunskog, Jonas; Cutanda Henriquez, Vicente; Jung, In-Jee; Ih, Jeong-Guon

Published in:
Proceedings of Inter-noise 2020

Publication date:
2020

Document Version
Publisher's PDF, also known as Version of record

Seoul inter-noise 2020 23-26 AUGUST

Experimental validation of a locally resonant metamaterial plate

Javier Hernan Vazquez Torre, Jonas Brunskog, Vicente Cutanda Henriquez[1]
Technical University of Denmark
Ørsteds Plads 352, 2800 Kongens Lyngby

In-Jee Jung, Jeong-Guon Ih[2]
Korea Advanced Institute of Science and Technology
291 Daehak-ro, Yusung-gu Daejeon 34141, Korea

ABSTRACT

An analytical model for broadband sound transmission loss of a finite single leaf wall using a metamaterial was previously developed and validated numerically. It is of interest to validate the analytical model with experimental results. In this paper, the band gap (BG) behavior of a locally resonant metamaterial is tested and compared to the analytical and numerical results. First, the unit cell resonance is measured for four nominally equivalent samples and the material properties extracted. Then, vibration analysis of a finite metamaterial plate is carried out. The influence of the variability of the properties of the resonators due to the construction method is analyzed both experimentally and numerically. Lastly, the result is compared to the analytical model and conclusions drawn. The analytical model could not be fully validated with the experimental measurements, but the specimen exhibited BG behavior. The variability of the resonators has an important influence in the performance of the metamaterial plate.

1. INTRODUCTION

Acoustic metamaterials (AM) are being studied extensively because of their novel properties not found in nature. The definition of acoustic metamaterials may be broadly interpreted as systems or materials that display (as a whole) extraordinary properties not found in natural materials with respect to sound and vibration characteristics, such as negative apparent mass and/or bulk modulus. [1–6]. They owe this behavior to internal subwavelength structures. One of the most important characteristics of the AM is the so-called band gaps (BG), a frequency region where wave propagation is not possible. This property shows great promise to be a good tool to be used in sound insulation, absorption, and even radiation [7–9]. Band gaps can be introduced into these structures by mounting an array of resonators to them. This type of construction has been studied and validated in recent years [1–6].

An analytical model for broadband sound transmission loss of a finite single leaf wall using a metamaterial was developed [9]. The analytical model is useful to better understand metamaterials composed of single degree of freedom resonators and how the different parameters affect their behavior. From the optimization process emerged the possibility of tuning the BG above the

[1]jhevaz@elektro.dtu.dk, jbr@elektro.dtu.dk, vcuhe@elektro.dtu.dk

[2]injee@kaist.ac.kr, j.g.ih@kaist.ac.kr

coincidence frequency as a tool to maximize the frequency range where the transmission loss of the metamaterial is larger than the bare plate. Numerical simulations validate the analytical model for the low frequency range where the wavelength of the wave traveling through the plate is much longer than the periodic distance between the resonators. It is of interest to validate the analytical model with experimental results.

In this paper, the band gap behavior of a locally resonant metamaterial plate is tested and compared to the analytical and numerical results. First, the unit cell resonance is measured and the material properties extracted. Then, vibration analysis of a metamaterial plate of 0.5 x 0.4 x 0.003 m is carried out. The influence of the variability of the properties of the resonators due to the construction method is analyzed. The importance of uncertainty quantification was researched and shown by Henneberg et al [10] and it is of great value to bridge the gap between theory and application in industry. Lastly, the result is compared to the analytical model and conclusions drawn.

2. METAMATERIAL DESCRIPTION

2.1. Theoretical model

Consider a finite thin plate with mass per unit area m_p'' lying in the $x-y$ plane coupled with an array of distributed resonators as seen in Fig. 1(a). The plate is located inside a rigid baffle at $z = 0$. For $z < 0$ the acoustic field consists of an incident plane wave p_i, a reflected plane wave p_r, and a scattered field p_s due to the motion of the finite wall. For $z > 0$ only the transmitted wave (p_t) is present. In this way, the acoustic field is split in two parts; the first considers an incident wave reflecting off of a rigid wall, and following a correction to take into account a baffled finite plate in the rigid wall through a scattering and transmission term. The wall is of size $a \times b$. It is important to note that, even though the plate considered is of finite size, there are no explicit boundary conditions in the formulation. The resonators are considered distributed and have mass per unit area m_r'', stiffness per unit area s'' and provide a reaction force per unit area F''(Fig.1(b)). Structural damping of the spring is considered by

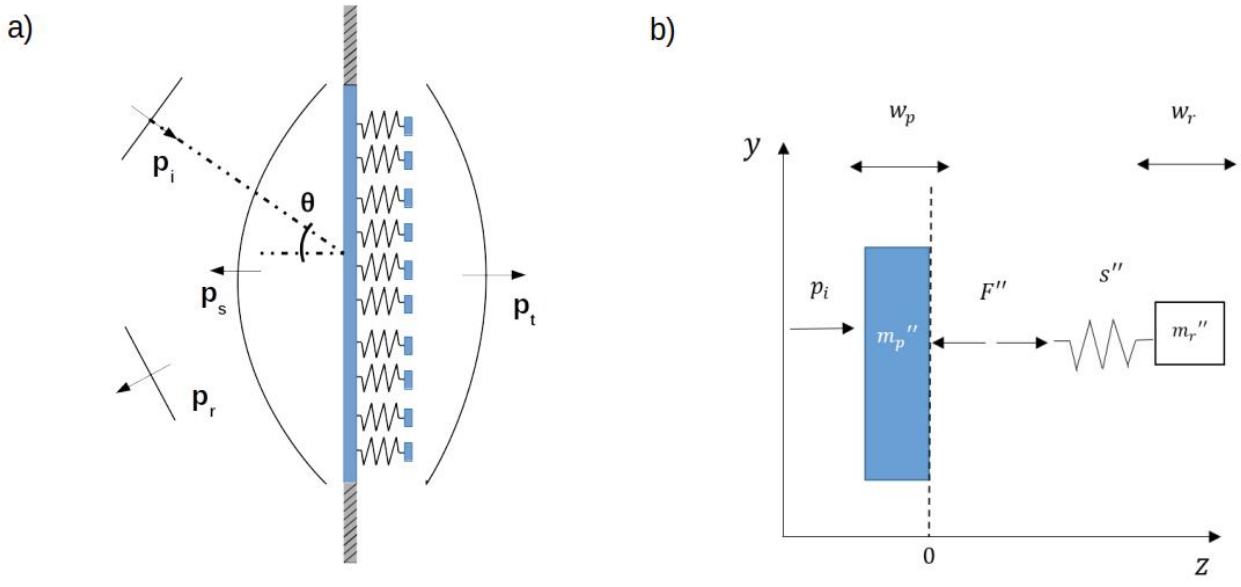

Figure 1: a) A finite wall of dimensions $a \times b$ coupled with a series of mass-spring resonators located inside a rigid baffle in the x-y plane, at z=0. b) Simplified diagram of a small section of the structure.

assigning the inherent losses to the spring element. For harmonic motion this can be represented by a complex stiffness $\underline{s}'' = s''(1 + i\eta_s)$ where η_s is the damping loss factor and s'' is the real part of the complex spring constant. Note that periodicity is not being explicitly assumed in the analytical model.

The reaction force per unit area of the distributed resonators is studied. This is a good approximation to the full problem in cases where the reflections at the boundary are of minor importance.

Starting from the forced Helmholtz equation for bending waves in plates it is possible to derive a modified Helmholtz equation that takes into account the effect of the coupled resonators. The result is shown in Equation 1 (the full derivation can be found in [9]),

$$\nabla^4 w_p - w_p \left(k_b^4 + \frac{m_r'' \omega^2 s''(1 + i\eta_s)}{B'[m_r''(\omega_0^2 - \omega^2) + i\eta_s s'']} \right) = \frac{p(x,y)}{B'}, \tag{1}$$

where $k_b = \sqrt[4]{\omega^2 m_p''/B'}$ is the wavenumber of the free bending wave in the plate, B' is the bending stiffness of the plate and $p(x,y) = p_i + p_r + p_s - p_t$ is the external pressure field. With this notation, $w_p(x,y)$ corresponds to traverse displacement of the plate. $\nabla^4 = \nabla^2\nabla^2$ is the bi-harmonic operator and ∇^2 is the Laplace operator. From Equation 1, the modified wavenumber can be identified as

$$k_{mod} = \sqrt[4]{k_b^4 + \frac{m_r'' \omega^2 s''(1 + i\eta_s)}{B'[m_r''(\omega_0^2 - \omega^2) + i\eta_s s'']}}. \tag{2}$$

This is an important expression because it determines the frequency range where wave propagation is not possible in the structure, commonly referred to as band gap. The modified wavenumber takes an imaginary value in this frequency range. If losses are not considered and after some modifications, an expression for the BG can be found

$$\omega_0 < \omega < \sqrt{\omega_0^2 + \frac{s''}{m_p''}}. \tag{3}$$

It is shown that the upper limit of the band gap is also related to the natural frequency of the resonators. The mass of the plate is an important factor in the band gap. From Equation 3, considering $s = \omega_0^2 m_r''$ and defining a mass ratio $M = m_r''/m_p''$ the width of the band gap can be expressed as

$$\Delta\omega_{BG} = \omega_0 \left(\sqrt{1 + M} - 1 \right). \tag{4}$$

As a result of this, it can be stated that the frequency width of the band gap grows with mass ratio M.

2.2. Numerical model

The numerical simulations carried out in this research were calculated using COMSOL Multiphysics® software [11]. The design chosen is presented in Fig. 2. The structure consists of an aluminium plate of 3 mm thickness with periodically added resonators in two dimensions. The resonator is made of a rubber spring (hardness 70 shore A) and a steel mass with dimensions $28 \times 28 \times 5$ mm and $30 \times 30 \times 10$ mm respectively. The unit cell is 50×50 mm and Floquet boundary conditions are used, assuming spatial periodicity (the numerical calculation is greatly simplified by just considering a single resonator and periodic conditions). Material properties are shown in table 1. The dynamic properties of rubber were extracted from experimental measurements detailed in Section 2.3. This design was chosen to get as close a possible to the conditions set in the analytical model, while defining a setup that is realizable in practice.

Dispersion curves are calculated along the irreducible Brillouin contour without losses [12, 13]. The eigensolver analysis is set up as a parametric sweep involving one parameter, k, which varies from 0 to 3. In this study, 0 to 1 defines a wave number spanning the $\Gamma - X$ edge, 1 to 2 defines a wave number spanning the $X - M$ edge, and 2 to 3 defines a wave number spanning the diagonal $M - \Gamma$ edge of the irreducible Brillouin zone (IBZ)(Fig. 3). For each value of k, it is solved for the lowest natural frequencies [14].

A finite metamaterial plate of 0.5 x 0.4 x 0.003 m is simulated in order to compare with the experimental measurements (Fig. 4). The measurement setup described in Fig. 5(b) and 7 is replicated in order to compare and match the results.

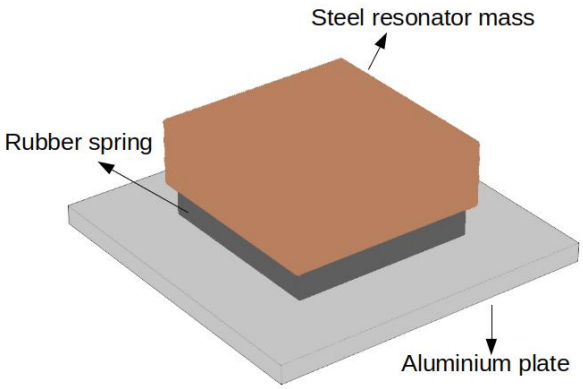

Figure 2: Unit cell used for validation (50×50 mm). Aluminium plate 3 mm thickness, $30 \times 30 \times 10$ mm steel mass and $28 \times 28 \times 5$ mm rubber spring (hardness 70 shore A).

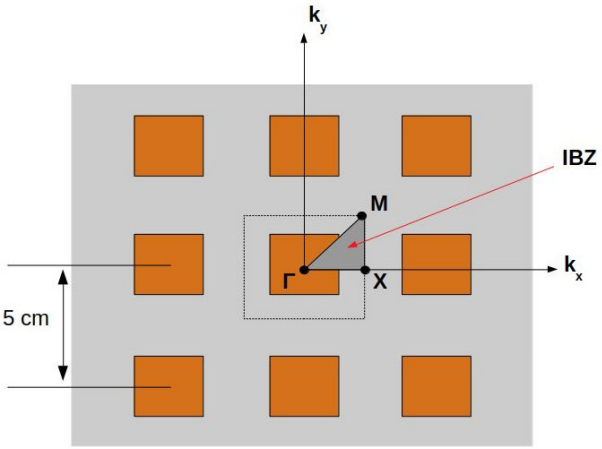

Figure 3: Diagram of the irreducible Brillouin zone used for the dispersion curves computation.

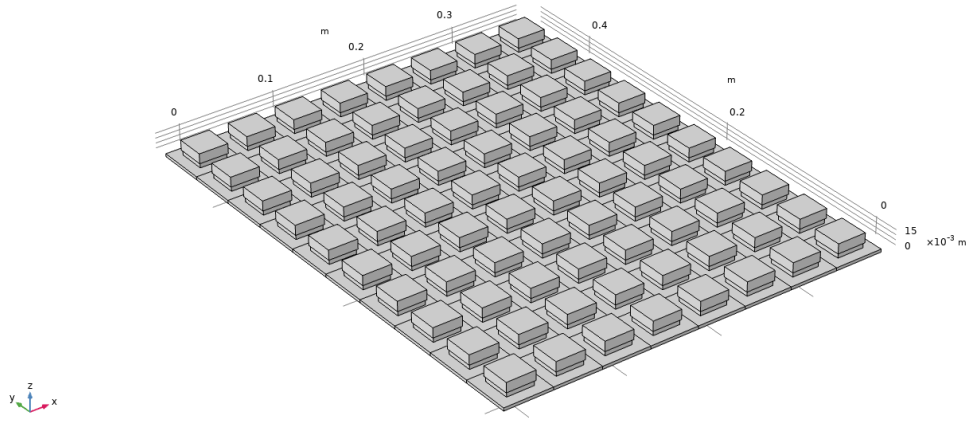

Figure 4: Numerical simulation of a finite metamaterial plate of 0.5 x 0.4 x 0.003 m.

Table 1: Material properties of structure.

Property	Aluminium	Rubber	Steel
Young's modulus	68×10^9 [Pa]	8.4×10^7 [Pa]	2×10^{11} [Pa]
Density	2670 [kg/m^3]	1530 [kg/m^3]	8000 [kg/m^3]
Poisson's ratio	0.33	0.4	0.28
Loss Factor	0.05	0.16	0.03

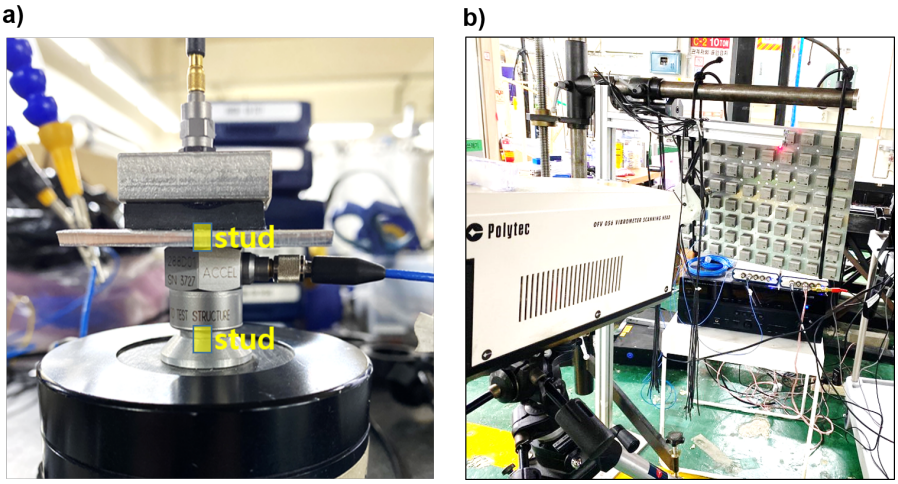

Figure 5: a) Unit cell measurement setup b) Metamaterial plate measurement setup.

2.3. Experimental model

The experimental model is constructed using an aluminium plate, steel mass and rubber springs as described in Section 2.2. The material properties of aluminium and steel are well known, but the dynamic properties of rubber are more difficult to estimate. Other factors like temperature, stress and the geometry itself can change the properties, making rubber an unreliable material for these resonators. On the other hand, rubber is easy to come by and relatively inexpensive. Furthermore, this setup was chosen to get as close as possible to the conditions set in the analytical model, given that the objective is to validate it. In order to extract the material properties of the rubber, 4 unit cells were constructed and measured for the resonance as shown in Fig. 5(a). An accelerometer is used to measure the velocity of the steel mass, while an impedance head measures the velocity in the excitation point where a shaker is connected to the aluminium plate. The input signal is a linear sine sweep, from 0 Hz up to 12 kHz. The transmissibility is calculated and results are shown in Fig. 6. The solid red curve is the Comsol simulation of the unit cell measurement. The material properties of the rubber were chosen to fit roughly to the average of the results and shown in table 1. The unit cells measured have different resonances and loss factors, possibly due to the construction methodology. The rubber was glued with epoxy to the steel mass and the aluminium plate. The amount of glue used was not consistent for all unit cells and the impact this may have in the properties of the rubber is unknown. Furthermore, the pieces have small size variations because of cutting errors. Nevertheless, the measured properties of the rubber are within the expected range for this type of material.

The metamaterial plate measurement setup is shown in Fig. 5(b). The test consists of 1 excitation point and 35 measurement positions. A shaker is used to excite the system with a sine sweep from 800 Hz to 6 kHz. The metamaterial plate is hanging from a lateral excitation stand, supported by 2 rubber bands. As a result, it has free boundary conditions. The shaker is connected to the plate with a drive rod, and a laser Doppler vibrometer (ldv) measures the input velocity from the back of the plate. The measurement positions are shown in Fig. 7 and also measured with the ldv. Then, the ratio of the

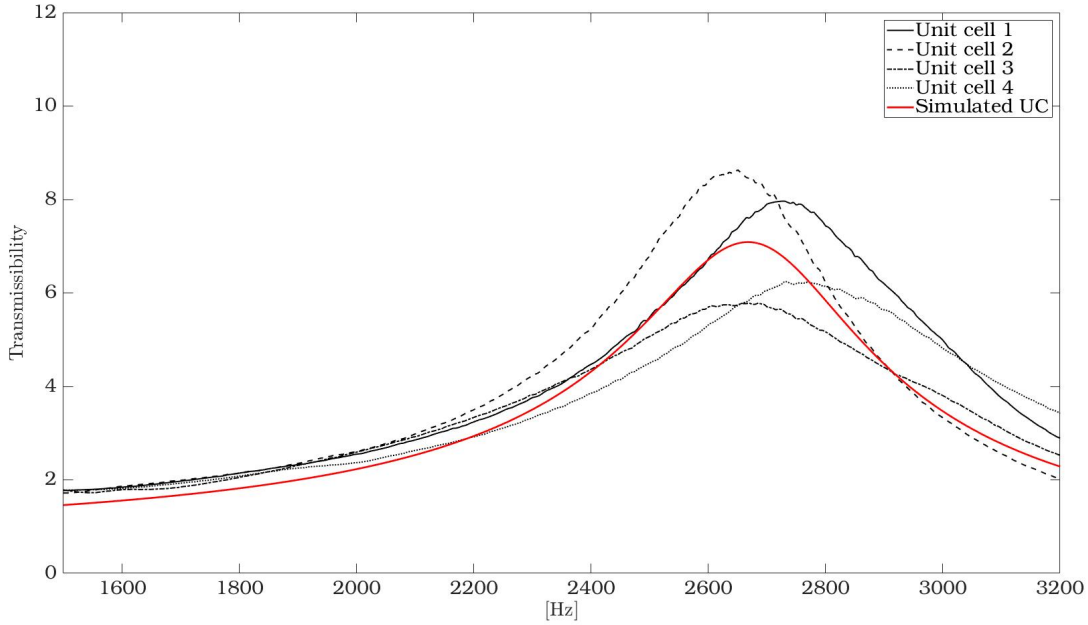

Figure 6: Unit cell measurement and Comsol simulation results.

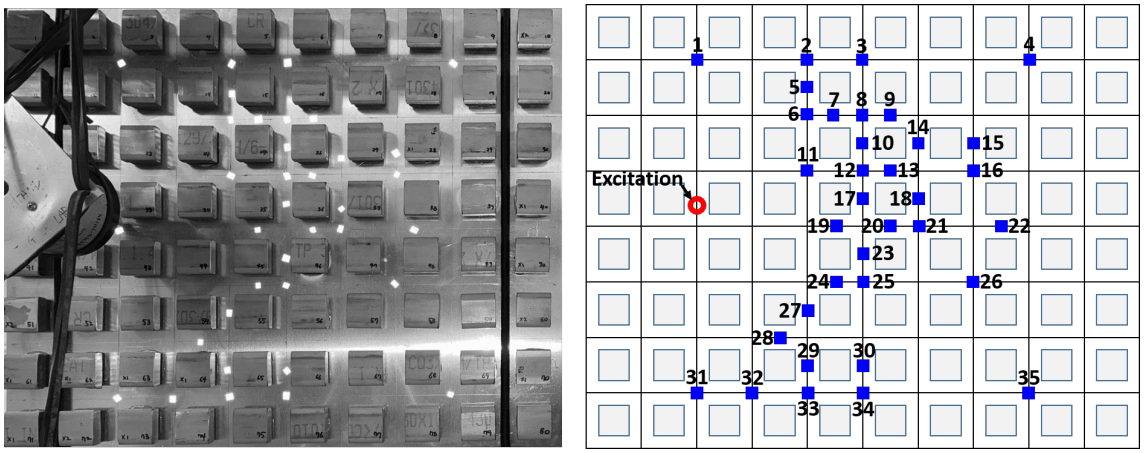

Figure 7: Measurement positions for the metamaterial plate test.

average absolute square velocity for all 35 positions to the absolute square velocity in the excitation point is calculated as

$$\overline{T} = 10log\frac{\overline{|v_m|^2}}{|v_e|^2}, \tag{5}$$

where v_m is the vibration velocity in the measurement positions and v_e is the velocity at the excitation point. The vibration velocity should be highly attenuated in the band gap region, making it easily identifiable from this result.

3. RESULTS AND ANALYSIS

The numerically determined periodic dispersion curve for the metamaterial plate described in Sec. 2 was calculated using the properties shown in table 1 but without damping. Results are presented in Fig. 8. The BG is located between 2315 Hz and 5759 Hz. and it is consistent with the approximations made in the analytical model as shown in [9]. According to the analytical model, the lower limit of the BG corresponds to the natural resonant frequency of the resonators, while the upper limit corresponds

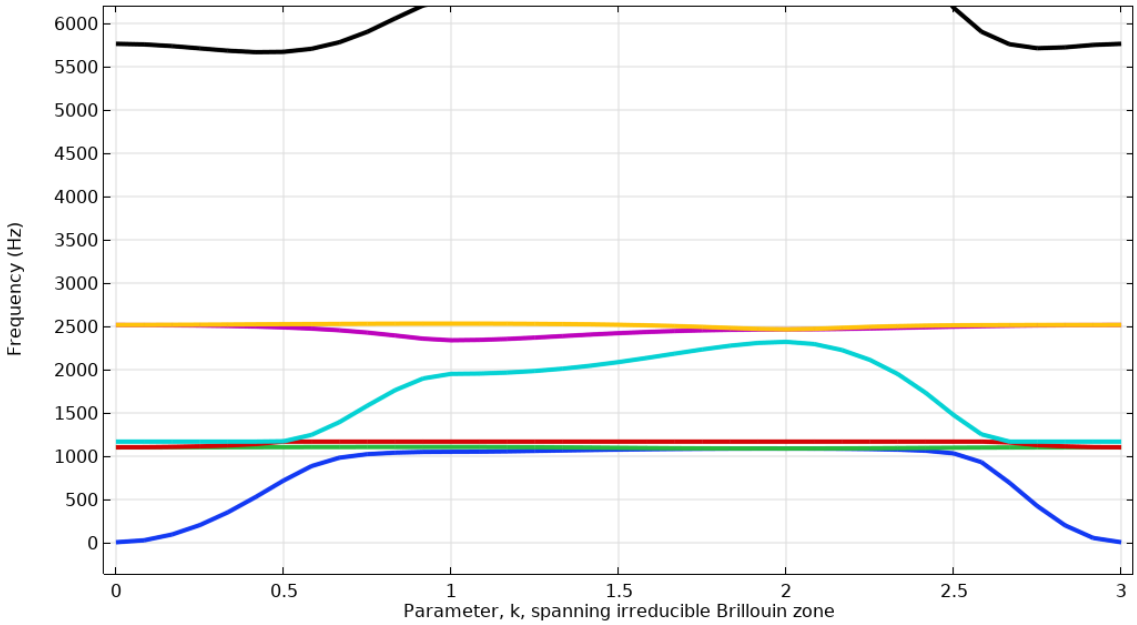

Figure 8: Numerically determined periodic dispersion curve for the metamaterial plate.

to the opposite case, when the mass of the resonators and the plate are out of phase. This is the case in the simulations. There are two rotational modes around 2.5 kHz that are not present in the analytical model given the assumptions made. These can be seen in Fig. 8 represented by the yellow and magenta lines that are mostly overlapping.

The results of the finite metamaterial plate measurement and the Comsol simulations are presented in Fig. 9. The properties used for the simulation are shown in table 1. The vertical dashed lines represent the frequency limits of the theoretical band gap following Eq. (3). It is clear that the measurement and simulation do not have a good fit in the frequency range of the BG. The simulation and band gap limits are calculated for an homogeneous case, where all resonators are equal, and in the case of the theoretical BG, for a simple one degree of freedom resonator without losses. The analytical BG and the simulation fit well together, but when compared to a real measurement differences arise. As described in Sec. 2.3, the constructed resonators are not equal. From the unit cell measurements it was seen that deviations in resonance frequency and loss factor exist. Furthermore, it is possible that the epoxy used to glue the parts together has hardened to the point of making the connection between the pieces rigid for this frequency range. To test this hypothesis, a simulation was carried out. Figure. 9 shows the comparison between the measured metamaterial plate and a simulation performed with the resonators following a normal distribution with standard deviation consistent with the UC measurements shown in Fig. 5. This means that the Young's modulus and loss factor of the rubber are different for every resonator. Moreover, the boundary between the rubber and steel mass is simulated as rigid in some of the resonators. The Rigid Connector is a boundary condition for modeling rigid regions in Comsol. A rigid connector can connect an arbitrary combination of boundaries, edges, and points which all will move together as being attached to a virtual rigid object. The result of this simulation shows a larger apparent BG than the homogeneous case, being more consistent with the measurement. The results are sensitive to all of these variables. Given the complexity and uncertainties present in this experiment, a mismatch between measurement and simulation is seen. The simulation with normal distribution indicates that the variability in the resonators and the effect of the epoxy in the rubber are a likely explanation for the mismatch. The measurement result seem to indicate the presence of a band gap nonetheless, but it is bigger and it starts at a lower frequency than expected.

Manufacturing tolerance is an important topic when trying to connect theory and industry applications. It was observed from the simulations in Fig. 9 that the variability in the resonance

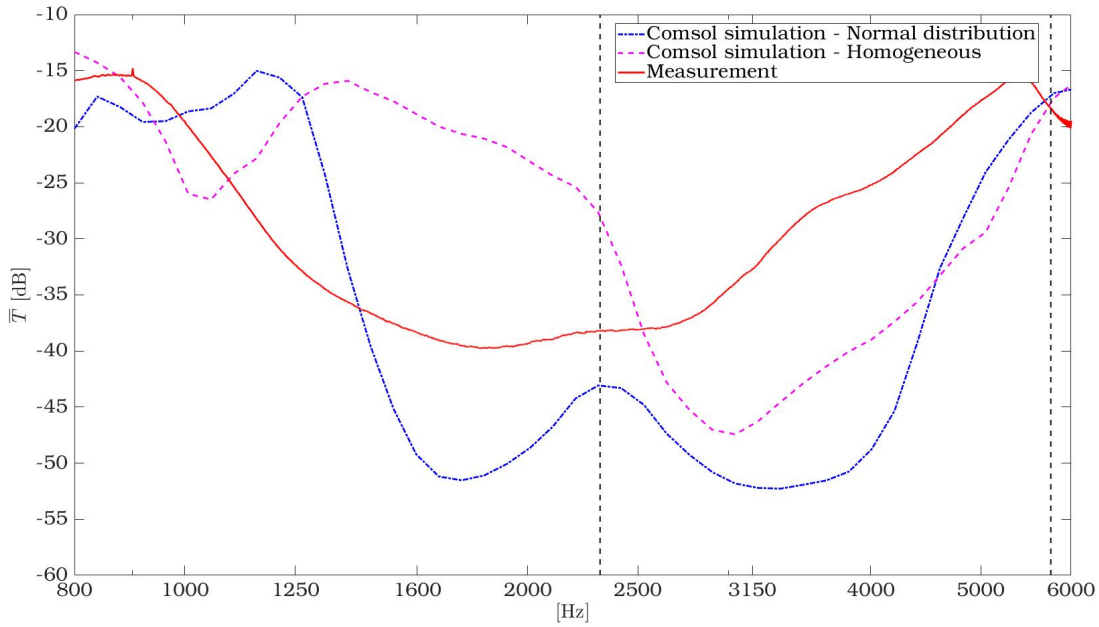

Figure 9: Metamaterial plate measurement results and Comsol simulations with homogeneous resonators and normal distribution. Vertical dashed lines represent the theoretical BG limits.

of the resonators is an important factor in the performance of the metamaterial plate. In order to better understand its influence, additional simulations were carried out. Figure 10 shows simulations of the measurement with normal distribution with different standard deviations compared to the homogeneous case. The homogeneous case is calculated with the properties presented in table 1. It is important to note that the loss factor is 0.16 for all simulations. The only stochastic variable is the Young's modulus of the rubber for each of the resonators, that follows a normal distribution. Additionally, the connection between the parts of the resonators is not simulated as rigid. The objective is to isolate the influence of the variability in the resonance. These results indicate that a small variation in the resonance frequency of the resonators of the metamaterial increases the damping of the average velocity of the structure when compared to the homogeneous case. This may be because of Anderson localization phenomena of nearly periodic structures [15]. It can be noted that this phenomena can have an apparent increased damping, which is beneficial for sound insulation [16]. If the standard deviation is large, the velocity response worsens considerably. Usually, variability in metamaterials is regarded as something unfortunate and negative, but the simulations shown in Fig. 10 indicate that it may not always be the case, possibly due to Anderson localization phenomena. Vibrations in the plate are more damped than in the homogeneous case. This can emerge as a new design tool when creating metamaterials. If the deviations are too great, the benefits shown disappear. It is left for future research a more comprehensive study of the influence of the uncertainties in the metamaterial behavior.

4. CONCLUSIONS

Vibration analysis was carried out in a locally resonant metamaterial plate in order to validate a previously developed analytical model. While the analytical model has been validated with numerical simulations, the experimental measurements yield inconclusive results. The uncertainties present in the construction of the specimen measured make the validation difficult. The measured metamaterial plate exhibits band gap behavior, but not in the same frequency range as the analytical and numerical simulations indicate. It appears to be a bigger BG and it starts at a lower frequency. The epoxy

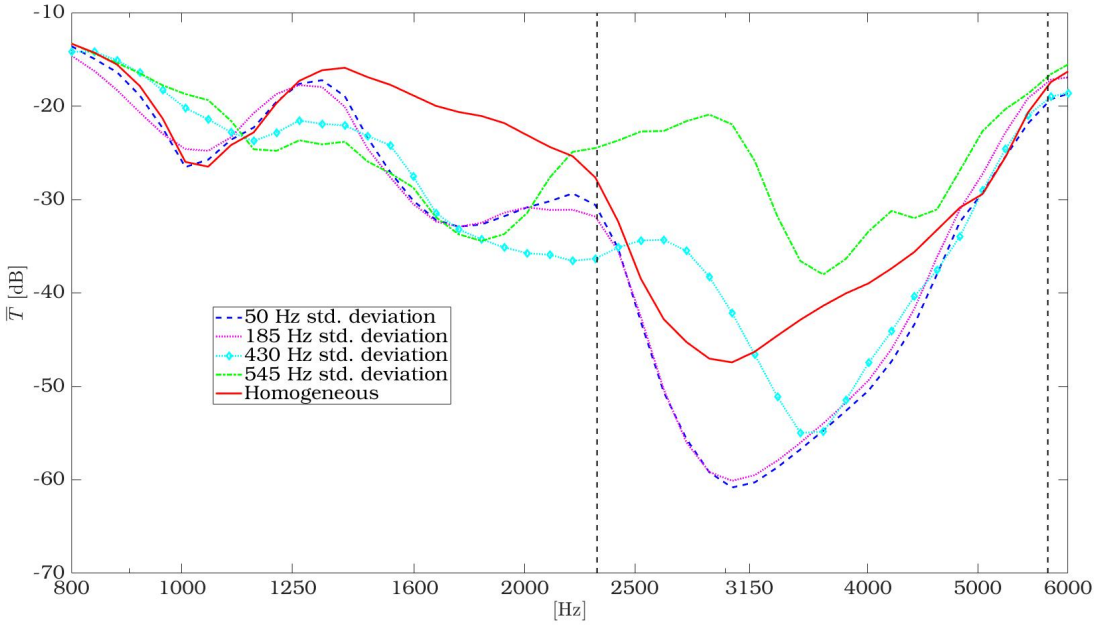

Figure 10: Simulations of the measurement with normal distribution of the resonators Young's modulus with different standard deviations compared to the homogeneous case. Vertical dashed lines represent the theoretical BG limits.

used to glue the parts of the resonators has an unknown effect in the properties and behavior of the metamaterial, making a direct comparison complex.

Even though the analytical model could not be fully validated with the experimental measurements, the specimen exhibited band gap behavior and in a similar frequency range. The variability shown by the resonators affects the results considerably, reassuring the importance of establishing manufacturing tolerances when designing these structures. Furthermore, from the analysis emerges the possibility of using the variability as a design tool in metamaterials.

5. ACKNOWLEDGEMENTS

This research was carried out within the Signature project, a collaboration between the Technical University of Denmark and the Korea Advanced Institute of Science and Technology in the research of metamaterials for sound insulation, radiation and absorption.

6. REFERENCES

[1] N. Sui, X. Yan, T.-Y. Huang, J. Xu, F.-G. Yuan, and Y. Jing, "A lightweight yet sound-proof honeycomb acoustic metamaterial," *Applied Physics Letters*, vol. 106, no. 17, p. 171905, 2015.

[2] S. H. Lee, C. M. Park, Y. M. Seo, Z. G. Wang, and C. K. Kim, "Acoustic metamaterial with negative density," *Physics Letters A*, vol. 373, no. 48, pp. 4464 – 4469, 2009.

[3] K. Lu, J. H. Wu, D. Guan, N. Gao, and L. Jing, "A lightweight low-frequency sound insulation membrane-type acoustic metamaterial," *AIP Advances*, vol. 6, no. 2, p. 025116, 2016.

[4] S. Li, D. Mao, S. Huang, and X. Wang, "Enhanced transmission loss in acoustic materials with micro-membranes," *Applied Acoustics*, vol. 130, pp. 92 – 98, 2018.

[5] N. Jiménez, W. Huang, V. Romero-García, V. Pagneux, and J.-P. Groby, "Ultra-thin metamaterial for perfect and quasi-omnidirectional sound absorption," *Applied Physics Letters*, vol. 109, no. 12, p. 121902, 2016.

[6] X. Wang, X. Luo, H. Zhao, and Z. Huang, "Acoustic perfect absorption and broadband insulation achieved by double-zero metamaterials," *Applied Physics Letters*, vol. 112, no. 2, p. 021901, 2018.

[7] J. Jung, C. H. Jeong, and J. S. Jensen, "Efficient sound radiation using a bandgap structure," *Applied Physics Letters*, vol. 115, 7 2019.

[8] J. Jung, H.-G. Kim, S. Goo, K.-J. Chang, and S. Wang, "Realisation of a locally resonant metamaterial on the automobile panel structure to reduce noise radiation," *Mechanical Systems and Signal Processing*, vol. 122, pp. 206 – 231, 2019.

[9] J. H. Vazquez Torre, J. Brunskog, and V. Cutanda Henriquez, "An analytical model for broadband sound transmission loss of a finite single leaf wall using a metamaterial," *The Journal of the Acoustical Society of America*, vol. 147, no. 3, pp. 1697–1708, 2020.

[10] J. Henneberg, J. G. Nieto, K. Sepahvand, A. Gerlach, H. Cebulla, and S. Marburg, "Periodically arranged acoustic metamaterial in industrial applications: The need for uncertainty quantification," *Applied Acoustics*, vol. 157, 2020.

[11] COMSOL Multiphysics® v. 5.4, COMSOL AB, Stockholm, Sweden.

[12] L. Brillouin, *Wave propagation in periodic structures*. New York: McGraw-Hill Book company, 1946.

[13] J. O. Vasseur, P. A. Deymier, A. Sukhovich, B. Merheb, A.-C. Hladky-Hennion, and M. I. Hussein, "Phononic band structures and transmission coefficients: Methods and approaches," in *Acoustic Metamaterials and Phononic Crystals* (P. A. Deymier, ed.), pp. 329–372, Berlin, Heidelberg: Springer Berlin Heidelberg, 2013.

[14] N. Elabbasi, "Modeling phononic band gap materials and structures," 2016.

[15] P. W. Anderson, "Absence of diffusion in certain random lattices," *Phys. Rev.*, vol. 109, pp. 1492–1505, Mar 1958.

[16] J. Brunskog, "Near-periodicity in acoustically excited stiffened plates and its influence on vibration, radiation and sound insulation," *Acustica United with Acta Acustica*, vol. 90, pp. 301–312, 2004.